ANNEALING TEMPERATURE AND COCATALYST EFFECTS TO THE PHOTOELECTROCHEMICAL PROPERTY OF CuInS2 THIN FILM SEMICONDUCTOR

by Gunawan Gunawan

Submission date: 14-Jun-2021 09:19AM (UTC+0700)
Submission ID: 1605950417
File name: Jurnal_rasayan_C46.pdf (1.85M)
Word count: 3650
Character count: 18641

RJC

RASĀYAN *J. Chem.*
Vol. 14 | No. 2 |1322-1329| April - June | 2021
ISSN: 0974-1496 | e-ISSN: 0976-0083 | CODEN: RJCABP
http://www.rasayanjournal.com
http://www.rasayanjournal.co.in

ANNEALING TEMPERATURE AND COCATALYST EFFECTS TO THE PHOTOELECTROCHEMICAL PROPERTY OF $CuInS_2$ THIN FILM SEMICONDUCTOR

Gunawan[1,✉], A. Haris[1], H. Widiyandari[2], D. S. Widodo[1], W. Septina[3] and S. Ikeda[4]

[1]Chemistry Department, Faculty of Science and Mathematics, Diponegoro University, Semarang-50271, Indonesia

[2]Physics Department, Faculty of Mathematics and Natural Sciences, Sebelas Maret University, Surakarta 57126, Indonesia

[3]Hawaii Natural Energy Institute University of Hawai'i at Mānoa (UHM), 1689 East West Road, POST 109 Honolulu, HI 96822, United States

[4]Department of Chemistry, Faculty of Science and Engineering, Konan University, 8-9-1 Okamoto, Higashinada-ku, Kobe 658-8501, Japan

✉Corresponding Author: gunawan@live.undip.ac.id

ABSTRACT

Thin film of $CuInS_2$ semiconductor had been synthesized by copper and indium stack electrodepositions on a molybdenum glass substrate and followed by sulfurization at varied annealing temperatures of 600-800 ºC. $CuInS_2$ thin film was characterized by using XRD, Raman, and SEM. Then on the $CuInS_2$ was deposited Pt with various deposition times and its photocurrent property was observed. Finally, Pt or Rh cocatalyst deposited on In_2S_3-$CuInS_2$ was also measured its photoelectrochemical property. XRD, Raman, and SEM data showed $CuInS_2$ had a different character with varied annealing temperatures. An annealing temperature of 680 ºC gave a maximum photocurrent of $CuInS_2$ as a photocathode. The introduction of cocatalysts increased the photocurrent, even for Rh cocatalyst gave a better-applied bias photon-to-current efficiency than Pt.

Keywords: Photocathode, $CuInS_2$, Cocatalyst, Photocurrent.

RASĀYAN *J. Chem.*, Vol. 14, No.2, 2021

INTRODUCTION

Photoelectrochemical (PEC) water splitting to produce hydrogen gas (H_2) by using sunlight is hoped to be an ideal and environmentally clean technology to replace fossil fuel sources which tend to reduce in the short years. This idea motivates the scientific community to find various materials and strategies for that purpose. Fujishima *et al.* as the pioneer of PEC water splitting applied photoanode of TiO_2 irradiated by using UV light.[1] The finding motivated researchers to find out various types of semiconductors and configurations of PEC devices to improve the efficiency of water reduction to produce hydrogen gas (H_2).[2-7]

Single absorber with a wide bandgap gives a low efficiency of PEC water splitting because it only works at UV light, therefore to improve the efficiency by harvesting all sunlight irradiation regions dual absorbers seem more promising. They consist of photoanode and photocathode electrodes that function as water oxidation and reduction, respectively. With this dual absorber system, researchers can be more flexible and optimal to focus on each electrode, so that it is possible to obtain a real splitting of water without bias by irradiation using sunlight to the absorbers.

Considering the absorber as the cathode part, the materials of Cu-based chacopyrite as a *p*-type semiconductor are promising candidate absorbers for producing H_2 evolution efficiently.[8-13] The compound of $CuInS_2$ is one of the most important chalcopyrite because it has an optimal value of the bandgap and high absorption coefficient, namely 1.5 eV and 10^4 cm^{-1}, respectively, that allowing it to utilize sunlight efficiently.[14] Moreover, low-cost electrodeposition and annealing methods of thin-film

http://dx.doi.org/10.31788/ RJC.2021.1425818

fabrication techniques enable to prepare $CuInS_2$ photoelectrodes with high structural and optical quality.[15-18] Surface modification of $CuInS_2$ using buffer layer of *n*-type and platinum introduction enhances the cathodic photocurrent and it is very important for a better separation of electrons and holes generated by illumination.[19] Platinum is the best cocatalyst until now to perform hydrogen evolution reaction by facilitating interfacial charge transfer reactions[20]. Meanwhile, for water reduction, the semiconductor surfaces as electrodes have no especially catalytic property due to their high photogenerated carrier recombination. As it is usually applied widely in solar cells by fabrication *p* and *n* types of semiconductors of Cu-based chalcopyrite (*p-n* junctions) the covering of *n*-type of buffer layer on photo absorbers increases the photocurrent of the photocathode.[21-24] In this study, we investigated the effect of annealing temperatures of $CuInS_2$ thin film, and insertion of cocatalyst of Pt or Rh on the surface of photocathode of In_2S_3 covered $CuInS_2$ to improve its photoelectrochemical property since limited previous works discussed these cases. Their works mainly correlated to the temperature annealing effect of $CuInS_2$ on the structural and morphological as well as optical properties.[25,26]

EXPERIMENTAL

Materials and Instrumentations

The chemicals used were $CuSO_4$, $InCl_3$, trisodium citrate, citric acid, acetone, KCN, $In_2(SO_4)_3$, thioacetamide, CH3COOH, H_2PtCl_6, $RhCl_3$, Na_2SO_4, $Eu(NO_3)_3$, NaH_2PO_4. All chemicals were bought from *Merck* and used without purification. Molybdenum glasses were purchased from Geomatec Ltd. Japan. For annealing and drying the Cu/In film used H_2S (5%) and N_2 gases, respectively.

Potentiostat (Hokuto Dento 110) was used for electrodeposition of copper, indium, platinum and rhodium. X-ray diffraction (XRD) was performed for analysis of crystalline structures of the $CuInS_2$ film using *PANalytical X Pert*^{3} *Powder* X-ray diffractometer (Cu Kα, Ni filter). The $CuInS_2$ thin film's morphology was analyzed by using a scanning electron microscope (SEM) JSM-6510LA Analytical at an acceleration voltage of 20 kV. Raman analyses were obtained by using Raman Spectrophotometer (Jasco NRC 3100 Laser) with an excitation laser at a wavelength of 532 nm. Photocurrent responses and PEC measurements of bare and modified $CuInS_2$ used potentiostat coupled with digital function generator at 0.3 Hz and Shutter Controller.

Electrodeposition of Cu/In on Molybdenum Glass

The electrodeposition was carried out from copper then continued with indium electrolyte solutions successively with Ag/AgCl, Pt–wire, and a Mo-covered glass substrate (0.7 cm x 1.0 cm) as a reference, counter and working electrodes, respectively. Copper electrolyte pH 2.38 contained 0.05M $CuSO_4$, 0.15M trisodium citrate, and 0.242M citric acid. While indium electrolyte contained 0.03M $InCl_3$, 0.242M citric acid, and 0.036M trisodium citrate. The electrodepositions were run for 7 and 15 min for copper and indium using potentiostat at potentials of -0.2 and -0.78 V, respectively.

Effect of Annealing Temperature of $CuInS_2$

As deposited Cu-In was converted to $CuInS_2$ by pre-annealing for 30 min at a temperature of 160 ºC in Ar gas with flow rate at 200 mL/min and annealing for 10 min under 200 mL/min of H_2S (5% H_2S) flow in a glass tube furnace. The annealing temperature was varied at a temperature from 600 until 800 ºC. Then the $CuInS_2$ was immersed in KCN (10%) for 2 min to remove excess of Cu_xS. Effect of annealing temperature of $CuInS_2$ was observed by photocurrent response measurements used potentiostat coupled with digital function generator at 0.3 Hz and Shutter Controller. Three electrodes containing Ag/AgCl electrode, Pt counter electrode and $CuInS_2$ as working electrode were immersed in 0.2M $Eu(NO_3)_3$ solution. The measurement was run by chopped 1.5 AM light radiation to the working electrode with a sweep potential from 0 until -0.45V and a scan rate of 10 mV/s. Analysis of Raman, XRD and SEM were applied to characterize the effect of varying temperatures on synthesized $CuInS_2$.

Effect of Pt Cocatalyst Deposition

Pt electrodeposition on bare-$CuInS_2$ films was done using 20 mL electrolyte consisting 1mM H_2PtCl_6 and 0.1M Na_2SO_4 in cylindric flask with a window. Then into the flask was inserted bare-$CuInS_2$

photocathode, Pt, and Ag/AgCl as working, counter, and reference electrodes, respectively. Pt was photoelectrodeposited on the working electrode at various deposition times using potentiostat under illumination. Photocurrent response was measured using a similar procedure as above.

Effect of Type of Cocatalysts

Before deposition of cocatalysts, bare-$CuInS_2$ film was covered with In_2S_3 by immersed in an electrolyte containing 0.025M indium sulfate, 100 mM thiacetamide and 100 mM acetic acid at 65 °C for 15 min. Then Pt or Rh was deposited on modified $CuInS_2$ with a similar procedure as above with concentration 1mM for 10 s. Photoelectrochemical properties were performed in 0.2 M NaH_2PO_4 solution using a similar instrument and parameter as photocurrent response measurement. APBE (applied bias photon-to-current efficiency) was evaluated using equation:

$$ABPE\ (\%) = J \times V_b \times 100/P_{AM1.5}$$

Where J is photocurrent (mA/cm^2), V_b is bias voltage (RHE scale), and $P_{AM1.5}$ is 1.5AM simulated radiation (100 mW/cm^2). While RHE is calculated as the following, $RHE = E_{Ag/AgCl} + 0.059xpH + 0.199$.

RESULTS AND DISCUSSION

Effect of Annealing Temperature of $CuInS_2$

Preparation of semiconductors of $CuInS_2$ by successive electrodeposition of Cu and In of the precursor was conducted by annealing as-deposited Cu/In in H_2S gas at a temperature of 600 until 800 °C. The obtained $CuInS_2$ then were examined their photocurrent responses in 0.2 M europium solution (as electron scavenging) with chopped illumination and the results are depicted in Fig.-1. The figure can be seen the maximum photocurrent around 12.2 mA/cm^2 at a potential of -0.4V for $CuInS_2$ annealed at 680 °C with a good dark current. There is an anomaly in the results of the photocurrent response at temperatures of 620 and 640 °C. However, the photocurrent response has a trend to be optimum at 680 °C and becomes decrease after that temperature; those are 5.8 and 5.2 mA/cm^2 at annealing temperatures of 750 and 800°C, respectively (Tabel-1). $CuInS_2$ annealed at 700 to 800 °C gave a bad dark current, since the dark current not flat. The good absorber semiconductor should have zero current when there is no light (at dark).

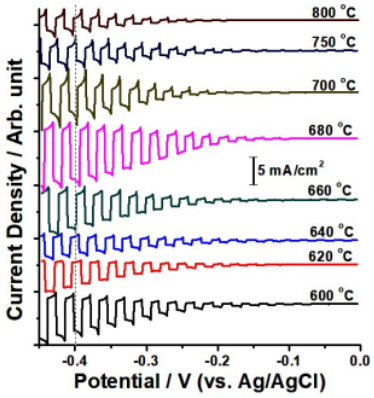

Fig.-1: Current-potential Curves of $CuInS_2$ measured using Potentiostat in Europium Solution under Chopped 1.5AM Simulated Radiation using Three-electrode systems.

Tabel-1: Photocurrent Response of $CuInS_2$ after Annealing at Varied Temperatures

Annealing Temperature (°C)	600	620	640	660	680	700	750	800
Photocurrent at Potential of -0.4 V (*vs.* Ag/AgCl) (mA/cm^2)	-8.1	-5.0	-3.8	-7.9	-12.2	-9.7	-5.8	-5.2

Figure-2 shows are typical $CuInS_2$ spectra at different annealing temperatures using Raman spectrophotometer. Raman shift at ca. 300 cm^{-1} is a typical peak for $CuInS_2$ and no other peaks appear for annealing temperatures until 680 °C. Whilst at annealing temperatures of 700 until 800 °C beside the peak of $CuInS_2$, there are other peaks of molybdenum element coming from molybdenum glass substrate used because the molybdenum was evaporated and deposited at the surface of $CuInS_2$ thin film when subjected to the temperatures. Therefore, it covered the surface of $CuInS_2$ confirmed by the low-intensity peaks of $CuInS_2$ thin films annealed at temperatures of 700, 750, 800 °C. The molybdenum has Raman shifts ca.321.8, 407.4, 453.4 cm^{-1}.

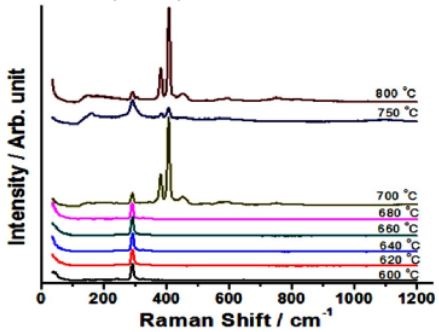

Fig.-2: $CuInS_2$ Raman Spectra annealed at Various Temperatures

The XRD spectra of $CuInS_2$ obtained from various annealing temperatures are shown in Fig.-3. The figure shows that at 2θ of 40.8° is the peak from molybdenum. While diffraction peaks at ca. 28.2, 46.8, and 55.4° are corresponding to the main crystalline chalcopyrite $CuInS_2$ phase. The values are almost close to the work of Bini *et al.*[27]

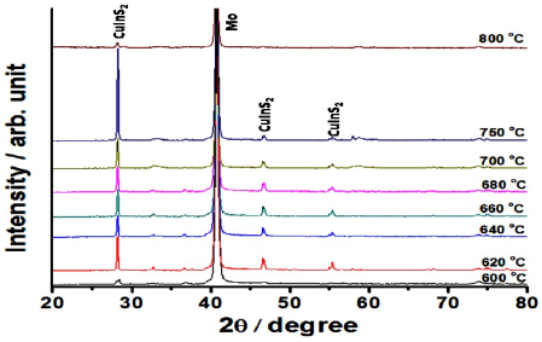

Fig.-3: XRD of $CuInS_2$ Obtained from Different Annealing Temperatures

Thin-film of $CuInS_2$ grain size was evaluated using formula of Debye-Scherrer, namely, $D = 0.9\ \lambda / \beta \cos\theta$. The values of D, λ, β, and θ are the diameter of the crystallites forming the film, wavelength of the CuKα line, FWHM and Bragg angle, respectively. The average grain sizes obtained from all peaks of $CuInS_2$ are in the range of 23 and 38 nm (Fig.-4). As the temperature increases, the grain size improves until temperature 640 °C with the highest grain size of 38.36 nm and after that, the grain size becomes decreases to 32.48 nm. As it is seen from Raman curve at higher annealing temperature (>700 °C) was not merely $CuInS_2$ present in the thin film. Since the $CuInS_2$ thin films prepared is almost pure, increasing temperature is effective until 640 °C, this is also confirmed by previous research that showed annealing temperature of $CuInS_2$ until the temperature of 550 °C.[28]

Figure-5 shows SEM of a thin film of $CuInS_2$ annealed at the temperatures of 600, 640, and 750 °C as a representation for three areas that have different grain sizes as shown in Fig.-4. The SEM shows that for $CuInS_2$ annealed at 600 °C has a porous property and small grain size, meanwhile the $CuInS_2$ annealed at

640 °C has a bigger grain size and also it looks like the film became melt. Although the decrease of grain size did not appear at an annealing temperature of 750 °C, the melted-like was disappeared. This can be due to the presence of molybdenum covered on its surface as confirmed by Raman measurement.

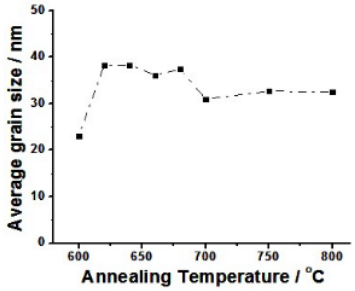

Fig.-4: Average Grain Size of a Thin Film of $CuInS_2$ at Various Annealing Temperatures

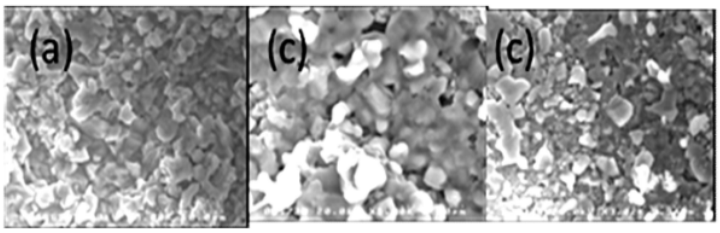

Fig.-5: SEM of $CuInS_2$ Annealed at Temperatures of 600, 640, and 750 °C

Effect of Pt cocatalyst Deposition

Platinum is a cocatalyst for hydrogen evolution reaction since it can bind with hydrogen ion to form ideal bond strength of Pt−H that can facilitate adsorption process and reduction of hydrogen ion and to release H_2 easily when reduction process is complete.[20] Figure-6 shows the deposition of Pt improves the photocurrent and onset potential compared with bare-$CuInS_2$. The photocurrent increases from 1.5 to 5 mA/cm^2 for bare and Pt deposited $CuInS_2$, respectively. While the onset potential gave more positive potential for Pt deposited $CuInS_2$ than bare-$CuInS_2$. However, the increase of deposition times (from 20 s until 1 h) has no significant effect on photocurrent as well as onset potential of Pt-$CuInS_2$.

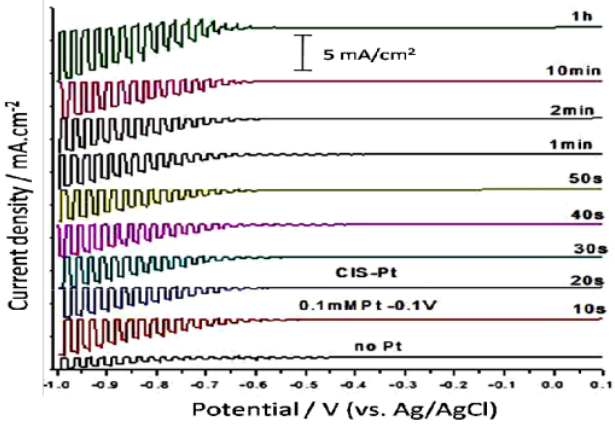

Fig.-6: Effect of Platinum Deposition Times on $CuInS_2$ to the Curves of Current-potential of Pt-$CuInS_2$ Photocathode measured in 0.1 M Na_2SO_4 at pH 9 under Chopped 1.5AM Simulated Radiation

Effect of Type of Cocatalyst

Effect of type of cocatalyst was evaluated using Rh as replacement of Pt. Since Pt has a work function a relatively large ca. 5.65 eV,[29] the formation of Schottky-type potential barrier would be possible that resists the transfer of electron. Therefore, Pt can be replaced by Rh as a candidate to reduce the potential barrier because of its relatively small work function (4.98 eV),[29] possible depositions by a photoelectron chemical method similar to that employed for the platinum deposition, and relatively low overpotential for water reduction comparable to that of Pt.[30,31] Figure-7a shows typical current and potential scans of Pt and Rh covered $In_2S_3/CuInS_2$ electrodes, respectively. The result shows appreciable improvement of photocurrent and also the onset potential achieved by using Rh catalyst for the $In_2S_3/CuInS_2$ electrode and improving the ABPE more than 2 % for Rh catalyst, as shown in Fig.-7b. Since there is no significant improvement when the Rh catalyst was used instead of the Pt catalyst for the $CdS/CuInS_2$ electrode system, the use of Rh should work well by a combination with In_2S_3 but not for CdS having a relatively negative conduction band minimum (CBM).[32] Figure-8 shows the energy diagram of $In_2S_3/CuInS_2$, Rh and Pt. The absolute and the electrochemical scales are given on the right side.

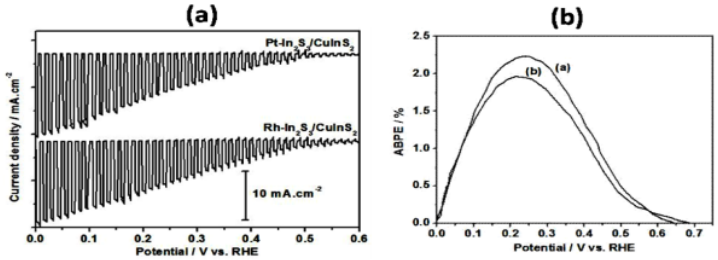

Fig.-7: (a) Current-potential Curves of Pt and Rh covered $In_2S_3/CuInS_2$ Photocathodes, respectively, in a Solution of 0.2 M NaH_2PO_4 at pH 6 with Chopped AM 1.5 Simulated Irradiation. (b) ABPE of Pt and Rh covered $In_2S_3/CuInS_2$ Photocathode, respectively.

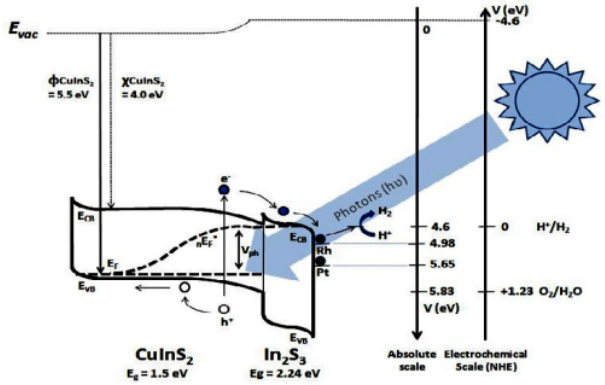

Fig.-8: Energy Diagram of $In_2S_3/CuInS_2$, Rh and Pt. The Absolute and the Electrochemical Scales are given on the Right Side.

CONCLUSION

$CuInS_2$ thin film had an optimum photocurrent response value of 12.2 mA/cm^2 when it was annealed at 680 °C. Deposition of platinum on $CuInS_2$ improved the photocurrent compared to bare $CuInS_2$. However, increasing times of Pt depositions had no significant effect on photoelectrochemical properties of the Pt-$CuInS_2$ photocathodes. Due to the relatively high CBM of the In_2S_3 photocathode layer, direct deposition of conventional Pt catalysts was found to be not optimal due to the generation of a large Schottky barrier; instead, the use of Rh was beneficial for this system, though it is still not sufficiently improved.

ACKNOWLEDGEMENT

Financial grant from Diponegoro University (Selain APBN DPA SUKPA LPPM Universitas Diponegoro-RPI-2, 2018) was acknowledged.

REFERENCES

1. A. Fujishima and K. Honda, *Nature*, **238(5358)**,37(1972), **DOI:**10.1038/238037a0
2. Z. Liu, J. Zhang and W. Yan, *ACS Sustainable Chemistry and Engineering*, **6(3)**, 3565(2018), **DOI:**10.1021/acssuschemeng.7b03894
3. J. Li, X. Jin, R. Li, Y. Zhao, X. Wang, X. Liu and H. Jiao, *Applied Catalysis B: Environmental*, **240**, (2019), **DOI:**10.1016/j.apcatb.2018.08.070
4. C. Liu, F. Wang, J. Zhang, K. Wang, Y. Qiu, Q. Liang and Z. Chen, *Nano-Micro Letters,* **10(2)**, 37(2018), **DOI:**10.1007/s40820-018-0192-6
5. S. Zhou, K. Chen, J. Huang, L. Wang, M. Zhang, B. Bai, H. Liu and Q. Wang, *Applied Catalysis B: Environmental,* **266**, 118513(2020), **DOI:**10.1016/j.apcatb.2019.118513
6. H. Wu, Z. Zheng, C. Y. Toe, X. Wen, J. N. Hart, R. Amal and Y. H. Ng, *Journal of Materials Chemistry A*, **8**, 5638(2020), **DOI:**10.1039/d0ta00629g
7. M. P. D. Parimala, M. S. Kumar and M.C. Rao, *Rasayan Journal of Chemistry*, **10(3)**, 825(2017), **DOI:**10.7324/RJC.2017.1031746
8. Q. Cai, Z. Liu, C. Han, Z. Tong and C. Ma, *Journal of Alloys and Compounds,* **795**, 319(2019), **DOI:**10.1016/j.jallcom.2019.04.312
9. D. Chen, Z. Liu, Z. Guo, W. Yan and M. Ruan, *Chemical Engineering Journal,* **381**, 122655(2020), **DOI:**10.1016/j.cej.2019.122655
10. N. Gaillard, D. Prasher, M. Chong, A. D. DeAngelis, K. Horsley, H. A. Ishii, J. P. Bradley, J. Varley and T. Ogitsu, *ACS Applied Energy Materials,* **2**, 5515(2019), **DOI:**10.1021/acsaem.9b00690
11. P. Endla, *Rasayan Journal of Chemistry,* **12(4)**, 1676(2019), **DOI:**10.31788/RJC.2019.1245132
12. Z. Liu, X. Lu and D. Chen, *ACS Sustainable Chemistry and Engineering,* **6(8)**, 10289(2018), **DOI:**10.1021/acssuschemeng.8b01607
13. V. Prasad, G. G. Simiyon, A. E. Mammen and N. Jayaprakash, *Rasayan Journal of Chemistry*, **12(2)**, 560(2019), **DOI:**10.31788/RJC.2019.1225226
14. M. A. Green, K. Emery, D. L. King, S. Igari and W. Warta, *Progress in Photovoltaics: Research and Applications*, **10(4)**,355(2002), **DOI:**10.1002/pip.453
15. M. Esmaeili-Zare and M. Behpour, *International Journal of Hydrogen Energy*, **45(32)**, 16169(2020), **DOI:**10.1016/j.ijhydene.2020.04.106
16. K. Maeba, Y. Matsuda, M. Takahashi, Y. Sakata, J. Zhang and S. Higashimoto, *Catalysis Today,* In Press (2020), **DOI:**10.1016/j.cattod.2020.01.015
17. C. An, F. Liu and J. Yuan, *Composite Interfaces,* 1–14(2020), **DOI:**10.1080/09276440.2020.1855572
18. S. Saber, M. Mollar, M., A. El Nahrawy, N. Khattab, A. Eid, M. Abo-Aly and B. Mari, *Optical and Quantum Electronics,* **50(6)**, 248(2018), **DOI:**10.1007/s11082-018-1521-1
19. B. Kim, K. Kim, Y. Kwon, W. Lee, W. H. Shin, S. Kim and J. Bang, *ACS Applied Nano Materials,* **1(6)**, 2449(2018), **DOI:**10.1021/acsanm.8b00250
20. Q. Cai, Z. Liu, C. Ma, Z. Tong and C. Han, *Journal of Materials Science: Materials in Electronics,* **29**, 20629(2018), **DOI:**10.1007/s10854-018-0201-z
21. Z. Chen, X. Liu, Y. Zhao, X. Liang, Y. Chen, L. Wang and Y. Shen, *Journal of Sol-Gel Science and Technology,* **85(1),** 12(2018), **DOI:**10.1007/s10971-017-4525-6
22. Y. Tani, K. Imada, T. Kamimura, M. Takahashi, M. Anpo and S. Higashimoto, *Research on Chemical Intermediates,* **47,** 169(2021), **DOI:**10.1007/s11164-020-04349-8
23. M. Li, R. Zhao, Y. Su, J. Hu, Z. Yang and Y. Zhang, *Applied Catalysis B: Environmental*, **203**, 715(2017), **DOI:**10.1016/j.apcatb.2016.10.051
24. T. Tomai, Y. Yasui, S. Watanabe, Y. Nakayasu, J. Sang, M. Sumiya, T. Momose and I. Honma, *The Journal of Supercritical Fluids*, **120**, 448(2017), **DOI:**10.1016/j.supflu.2016.05.026

25. P. Dube, A. O. Juma and C. M. Muiva, *Ceramics International,* **46(6)**, 7396(2019), **DOI:**10.1016/j.ceramint.2019.11.235
26. J. P. Sawant, R. J. Deokate, H. M. Pathan and R. B. Kale, *Engineered Science*, **13**, 51(2021), **DOI:**10.30919/es8d1147
27. S. Bini, K. Bindu, M. Lakshmi, C. S. Kartha, K. Vijayakumar, Y. Kashiwaba and T. Abe, *Renewable Energy,* **20(4)**, 405(2000), **DOI:**10.1016/S0960-1481(99)00122-6
28. R. Brini, M. Kanzari, B. Rezig and J. Werckmann, *European Physical Journal Applied Physics,* **30(3)**, 153(2005), **DOI:**10.1051/epjap:2005031
29. S. Wei, and A. Zunger, *Applied Physics Letters*, **63(18)**, 2549(1993), **DOI:**10.1063/1.110429
30. A. Niemegeers, M. Burgelman and A. De Vos, *Applied Physics Letters*, **67(6)**, 843(1995), **DOI:**10.1063/1.115523
31. Y. Hashimoto, K. Takeuchi, and K. Ito, *Applied Physics Letters*, **67(7),** 980(1995), **DOI:**10.1063/1.114965
32. Gunawan, W. Septina, T. Harada, Y. Nose, and S. Ikeda, *ACS Applied Materials and Interfaces*, **7(29)**, 16086(2015), **DOI:**10.1021/acsami.5b04634

[RJC-5918/2020]

ANNEALING TEMPERATURE AND COCATALYST EFFECTS TO THE PHOTOELECTROCHEMICAL PROPERTY OF CuInS2 THIN FILM SEMICONDUCTOR

ORIGINALITY REPORT

10%	7%	9%	3%
SIMILARITY INDEX	INTERNET SOURCES	PUBLICATIONS	STUDENT PAPERS

PRIMARY SOURCES

1	pubs.rsc.org Internet Source	2%
2	dyuthi.cusat.ac.in Internet Source	1%
3	www.bml.csiro.au Internet Source	1%
4	Yanwen Wang, Rong Liang, Chao Qin, Lei Ren, Zhizhen Ye, Liping Zhu. "Solution Processed Sb2S3-based Photocathode with Enhanced Photocatalytic Performance via Constructing Ultrathin TiO2 Overlayer and Noble Metal Modification", Sustainable Energy & Fuels, 2021 Publication	1%
5	Sudhanshu Shukla, Damilola Adeleye, Mohit Sood, Florian Ehre et al. " Carrier recombination mechanism and photovoltage deficit in 1.7-eV band gap near-stoichiometric Cu(In,Ga) ", Physical Review Materials, 2021	1%

Publication

6	Submitted to Pandit Deendayal Petroleum University Student Paper	1 %
7	Ikuo Ushiki, Yoshiyuki Sato, Shigeki Takishima, Hiroshi Inomata. "Thermodynamic Modeling of the Solubility of Acetylacetonate-Type Metal Precursors in Supercritical Carbon Dioxide Using the PC-SAFT Equation of State", JOURNAL OF CHEMICAL ENGINEERING OF JAPAN, 2019 Publication	<1 %
8	Maryam Hashemi, Seyed Mohammad Bagher Ghorashi, Fariba Tajabadi, Nima Taghavinia. "Investigation of precursors concentration in spray solution on the optoelectronic properties of CuInSe2 thin films deposited by spray pyrolysis method", Journal of Materials Science: Materials in Electronics, 2020 Publication	<1 %
9	Yinsi Wang, Yujie Liang, Dong Zeng, Min Zhu, Junli Fu, Tianyu Zhu, Hongsong Han, Cheng Li, Wenzhong Wang. "Electrochemical deposition of p-type β-Ni(OH)2 nanosheets onto CdS nanorod array photoanode for enhanced photoelectrochemical water splitting", Electrochimica Acta, 2020 Publication	<1 %

10	aip.scitation.org Internet Source	<1 %
11	Erik C. Neyts, Kostya (Ken) Ostrikov, Mahendra K. Sunkara, Annemie Bogaerts. "Plasma Catalysis: Synergistic Effects at the Nanoscale", Chemical Reviews, 2015 Publication	<1 %
12	Yuki Tani, Keiichiro Imada, Tomosumi Kamimura, Masanari Takahashi, Masakazu Anpo, Shinya Higashimoto. "Solution-processed fabrication of copper indium sulfide (CuInS2) as optical absorber for superstrate CuInS2/CdS/TiO2 solid-state solar cells", Research on Chemical Intermediates, 2021 Publication	<1 %
13	www.mdpi.com Internet Source	<1 %
14	Roy, J., and S. Maitra. "Mullitization of aluminosilicate diphasic gel in the presence of nickel oxide additive", Journal of Composite Materials, 2015. Publication	<1 %
15	rphysap.journaldephysique.org Internet Source	<1 %
16	www.human.cornell.edu Internet Source	<1 %

17	Lorenzo Rovelli, S. David Tilley, Kevin Sivula. " Optimization and Stabilization of Electrodeposited Cu ZnSnS Photocathodes for Solar Water Reduction ", ACS Applied Materials & Interfaces, 2013 Publication	<1 %
18	M. Morkel. "Flat conduction-band alignment at the CdS/CuInSe[sub 2] thin-film solar-cell heterojunction", Applied Physics Letters, 2001 Publication	<1 %
19	Shaoce Zhang, Zhifeng Liu, Mengnan Ruan, Zhengang Guo, Lei E, Wei Zhao, Dan Zhao, Xiangfeng Wu, Daimei Chen. "Enhanced piezoelectric-effect-assisted photoelectrochemical performance in ZnO modified with dual cocatalysts", Applied Catalysis B: Environmental, 2020 Publication	<1 %
20	link.springer.com Internet Source	<1 %
21	samurai.nims.go.jp Internet Source	<1 %
22	www.uosahiwal.edu.pk Internet Source	<1 %

Exclude quotes	Off	Exclude matches	Off
Exclude bibliography	Off		

ANNEALING TEMPERATURE AND COCATALYST EFFECTS TO THE PHOTOELECTROCHEMICAL PROPERTY OF CuInS2 THIN FILM SEMICONDUCTOR

GRADEMARK REPORT

FINAL GRADE

/0

GENERAL COMMENTS

Instructor

PAGE 1

PAGE 2

PAGE 3

PAGE 4

PAGE 5

PAGE 6

PAGE 7

PAGE 8